Aggressive Natural Killer-Like T-Cell Malignancy With Leukemic Presentation Following Solid Organ Transplantation

Yasodha Natkunam, MD, PhD, Roger A. Warnke, MD, James L. Zehnder, MD, and P. Joanne Cornbleet, MD, PhD

Key Words: Immunosuppression; Large granular lymphocytes; NK cells; NK-like T-cell leukemia; NK-like T-cell lymphoma; Posttransplant lymphoproliferative disorder

Abstract

NK-like T-cell malignancies are part of a spectrum of lymphoproliferative diseases that complicate immunosuppression associated with solid organ transplantation. We describe 2 patients with long-standing immunosuppression following solid organ transplantation. Both patients had systemic symptoms that included fever, myalgia, and weight loss. Organ involvement and lymphadenopathy were not initially observed. Unique to these 2 cases are the initial leukemic symptoms, which led to further characterization and identification of NK-like T-cell malignancies. Both patients exhibited an anomalous T/NK phenotype, CD56 positivity, and atypical blastic architecture of the large granular lymphocytes. Clonal rearrangement of T-cell receptor genes was detected in both patients. In 1 patient, a cytogenetic abnormality involving 8q24 was demonstrated. The disease course in both patients was aggressive, with involvment of multiple sites and rapid demise. This study emphasizes the importance of including NK-like T-cell malignancies in the differential diagnosis of lymphoproliferative disorders associated with immunosuppression and recognizing that an aggressive clinical course may follow leukemic presentation of disease.

Secondary malignancies are an important cause of morbidity and mortality after organ transplantation. The wide variety of secondary neoplasms described include non-Hodgkin's lymphoma, Hodgkin's disease, acute leukemias, and carcinomas. Among lymphoid malignancies occurring after transplantation, B-cell neoplasms account for approximately 80%. These posttransplantation lymphoproliferative disorders (PTLDs) form a morphologically heterogeneous spectrum that ranges from polyclonal or oligoclonal B-cell proliferations to malignant lymphoma.[1–5] The vast majority of B-cell PTLDs are associated with Epstein-Barr virus (EBV).[2]

T-cell PTLDs have also been described and account for approximately 14% of malignant lymphomas occurring after transplantation.[6] A subset of these T-cell proliferations harbor EBV.[7–9] Extranodal $CD3^+$ and $CD56^+$ T-cell lymphomas have been described in 4 patients with long-standing immunosuppression and organ transplantation.[10] These NK-like T-cell lymphomas were seen with widespread disease including hepatosplenic tumors with variable involvement of skin, lymph nodes, and peripheral blood. This study suggests that NK-like T-cell lymphoproliferative malignancies are part of the differential diagnosis of neoplasia in patients with immune system compromise.

We describe the clinical, cytologic, histologic, immunophenotypic, and cytogenetic findings in 2 patients with a history of chronic immunosuppression following solid organ transplantation who had NK-like T-cell leukemia. Both patients had systemic symptoms and circulating atypical large granular lymphocytes (LGLs). Progression to disseminated disease was rapid, and both patients died within weeks to months of initial work-up. Our observations suggest that the atypical cytologic findings of peripheral blood LGLs

together with the immunophenotype may predict an aggressive clinical outcome.

Case Reports

Case 1

The patient was a 40-year-old white woman who had received a heart-lung transplant 7 years previously because of primary pulmonary hypertension. Maintenance therapy included the immunosuppressant agents prednisone, azathioprine (Imuran), and cyclosporin. The postoperative course was relatively benign, complicated only by mild low-grade rejection (bronchiolitis obliterans). She was admitted to the hospital after having symptoms for 3 weeks that were attributed to viral infection and included productive cough, fever, myalgias, and headache. On admission, pancytopenia was noted. Initial hematologic data included WBC count $3,600 \times 10^3/\mu L$ ($3.6 \times 10^9/L$), hemoglobin level 8.0 g/dL (80 g/L), mean corpuscular volume 107 μm^3 (107 fL), and platelets $111 \times 10^3/\mu L$ ($111 \times 10^9/L$). The WBC count with slide differential showed 27% polymorphonuclear neutrophils, 22% band neutrophils, 10% lymphocytes, 9% monocytes, and 32% large blastic forms with nuclear folding and basophilic cytoplasm, some with azurophilic granules. Bone marrow examination revealed infiltration by neoplastic cells similar to those on the blood film. During her hospital course, severe respiratory distress developed secondary to alveolar hemorrhage. The patient's respiratory condition, renal and liver function, and mental status rapidly deteriorated, and she died 11 days after admission. Significant autopsy findings included bronchiolitis obliterans, transplant aortic and coronary arteriopathy, extramedullary glomerular sclerosis (cyclosporin effect), acute hemorrhagic pancreatitis, hepatosplenic congestion, necrotic spleen (accelerated postmortem autolysis secondary to pancreatitis), hypercellular marrow with immature cell forms, adrenal cortical atrophy, and osteoporosis. No tumor was identified in tissues other than bone marrow.

Pertinent investigations for infectious agents included cultures for bacteria and fungi (blood, urine, CSF, bronchoalveolar lavage [BAL], bone marrow), *Cryptococcus* antigen (blood, CSF), cytomegalovirus ([CMV] blood, BAL, bone marrow), stool pathogens, CMV IgM antibody, and human T-cell leukemia virus (HTLV) antibody-1; polymerase chain reaction (PCR) amplification for CMV (BAL); direct immunofluorescence examination and culture for respiratory syncytial virus and influenza types A and B (BAL); and parvovirus dot blot DNA hybridization (bone marrow).

Case 2

The patient, a 51-year-old white woman, had received a cadaver kidney transplant 24 years previously because of end-stage lupus nephritis. Maintenance therapy included the immunosuppressant agents azathioprine and prednisone. Splenectomy and bilateral nephrectomy were performed at transplantation. The posttransplantation course was complicated by 2 episodes of pneumonia, and sinusitis and urinary tract infections, but was otherwise unremarkable. At a routine clinic visit, the WBC count was $12,600 \times 10^3/\mu L$ ($12.6 \times 10^9/L$), hemoglobin level 6.7 g/dL (6.7 g/L), mean corpuscular volume 69.8 μm^3 (69.8 fL), and platelets $568 \times 10^3/\mu L$ ($568 \times 10^9/L$). Slide differential showed 35% polymorphonuclear neutrophils, 7% lymphocytes, 4% monocytes, and 53% atypical lymphoid cells, with high nuclear-cytoplasmic ratio, markedly irregular nuclear profiles, and coarse azurophilic cytoplasmic granules. A bone marrow biopsy specimen contained atypical lymphoid cells similar to those in the peripheral blood. Azathioprine was discontinued, and the prednisone dosage was tapered in an attempt to achieve remission. Staging work-up also revealed a nonocclusive thrombus in the right pulmonary artery, and warfarin sodium (Coumadin) therapy was initiated. Two months later, the patient had malaise, anorexia, nausea, and vomiting, and had lost 20 lb. A CT scan showed multiple nodular opacities in both lung fields. Intractable gastrointestinal bleeding developed suddenly. An exploratory laparotomy was performed, and a segment of proximal jejunum with multiple tumor nodules was resected. A trial course of chemotherapy with CHOP (cyclophosphamide, hydroxydaunomycin [doxorubicin], vincristine [Oncovin], and prednisone) was initiated, after which severe neutropenia and gram-negative sepsis developed. The patient's condition continued to deteriorate, and she died within 3 months of initial presentation. A postmortem examination was not performed, and we were unable to determine whether the radiographically detected opacities in the bilateral lung fields were due to lymphoma and whether other organ systems were involved at the time of death.

Pertinent studies for infectious agents included cultures for bacteria and fungi, and HTLV-1 (blood); immunoperoxidase studies for cytomegalovirus; and in situ hybridization for human herpesvirus (HHV) 8.

Materials and Methods

Morphology

Smeared cells from peripheral blood and bone marrow aspirate were stained with Wright-Giemsa. Bone marrow core biopsy specimens were fixed in Bouin solution, embedded in paraffin, and stained with H&E. Sections of the jejunum were fixed in 10% formalin, embedded in paraffin, and stained with H&E.

Flow Cytometry

Direct dual-parameter flow cytometry was performed (FACScan flow cytometer; Becton Dickinson, San Jose, CA)

with standard whole blood lysis or marrow mononuclear cells isolated at discontinuous gradient centrifugation with Ficoll-Hypaque (Pharmacia, Uppsala, Sweden). Commercially available fluorescein isothiocyanate (FITC)–conjugated or phycoerythrin-conjugated monoclonal antibodies were used **Table 1**. An analysis gate was selected to include the predominant population in the low forward–low side light scatter region. The percentage of events reactive with each monoclonal antibody was determined, setting thresholds with isotypic controls. Positive expression was defined as ≥20%.

Immunohistochemistry

Serial sections 4-µm thick were pretreated with a microwave procedure in citric acid buffer (10 mmol/L, pH 6.0) for 10 minutes before staining for CD3, CD20, and CD56. Endogenous peroxidase was blocked by preincubation with 1% hydrogen peroxide in phosphate-buffered saline solution. CD3 and CD20 staining was performed with an automated staining machine (Ventana Medical Systems, Tucson, AZ). Immunohistochemical stains for CD56 and CD57 were performed with a modified biotin-streptavidin method.[11] Primary antibodies were directed against CD3 (polyclonal, T cell; DAKO, Carpinteria, CA), CD20 (L26, B cells; DAKO), CD56 (123C3, NK cells, T-cell subset; Monosan, Uden, The Netherlands), and CD57 (Leu-7, NK cells, T-cell subset; Becton Dickinson).

Immunohistochemistry to demonstrate the presence of cytoplasmic CD3 was performed using cytocentrifuged slides prepared from Ficoll-Hypaque blood or bone marrow cell isolates. Slides were fixed for 30 seconds at room temperature in formalin-methanol-acetone (1:4:35) and washed with TRIS-buffered saline solution. After a 10-minute blocking step with TRIS-buffered saline solution–10% rabbit serum, the slides were incubated with a 1:10 dilution of CD3-FITC (Leu-4) or mouse IgG1-FITC (Becton Dickinson) for 60 minutes, then incubated for 15 minutes sequentially with biotinylated horse antimouse antibody (Vector Laboratories, Burlingame, CA), streptavidin-alkaline phosphatase (DAKO), and alkaline phosphatase substrate–chromogen reagent (DAKO). All incubations were performed at room temperature, and TRIS-buffered saline solution washes followed each incubation step.

Terminal deoxynucleotidyl transferase was assessed with an indirect immunofluorescent assay (Supertechs, Bethesda, MD).

Table 1
Monoclonal Antibody Reagents

Antibody	Clone	Source*	Major Cell Specificity
CD2	S5.2	Becton Dickinson	T, NK
CD3	SK7	Becton Dickinson	T
CD4	SK3	Becton Dickinson	T-helper, monocyte
CD5	L17F12	Becton Dickinson	T
CD7	4H9	Becton Dickinson	T, NK
CD8	SK1	Becton Dickinson	T-cytotoxic/suppressor
CD10	W8E7	Becton Dickinson	B-precursor
CD11c	S-HCL-3	Becton Dickinson	Myelomonocyte, NK
CD13	L138	Becton Dickinson	Myelomonocyte
CD14	MPO9	Becton Dickinson	Monocyte
CD16	3G8	Coulter/Itek	Myelomonocyte, NK
CD19	J4.119	Coulter/Itek	B
CD20	L27	Becton Dickinson	B
CD33	P67.6	Becton Dickinson	Myelomonocyte
CD34	HPCA-2	Becton Dickinson	Progenitor
CD45	HI30	Caltag	Pan-leukocyte
CD56	MY31	Becton Dickinson	NK, T-cytotoxic
CD57	HNK-1	Becton Dickinson	NK, T-cytotoxic
DR	L243	Becton Dickinson	B, activation antigen
βF1	WT31	Becton Dickinson	TCR-αβ heterodimer
TCR-δ-1	11F2	Becton Dickinson	TCR-γδ heterodimer

NK = natural killer; TCR = T cell receptor.
*Becton Dickinson, San Jose, CA; Coulter/Itek, Hialeah, FL; Caltag, Burlingame, CA.

In Situ Hybridization for Epstein-Barr Virus *EBER1* RNA

Epstein-Barr virus RNA in situ hybridization studies were performed using a 30-base oligonucleotide probe complementary to a portion of the *EBER1* gene, as previously described.[12] Paraffin sections 5-µm thick were deparaffinized, rehydrated, predigested with proteinase K, and hybridized overnight at a concentration of 0.25 ng/µL of biotinylated probe. Detection was accomplished with streptavidin–alkaline phosphatase conjugate. For each assay, known EBV-positive neoplasm served as a positive control, and EBV-negative lymphoid tissue as a negative control.

Cytogenetic Analysis

For chromosome analyses, bone marrow aspirate was cultured and chromosomes were analyzed with the GTW banding method.[13] Twenty chromosome metaphases were analyzed in patient 1, but only 4 metaphases were available for analysis in patient 2.

Southern Blot Analysis

High molecular weight DNA samples were extracted using phenol-chloroform, precipitated in ethanol, cleaved with restriction enzymes, fractionated according to size by agarose gel electrophoresis, denatured, and transferred to nylon membranes. Hybridization using phosphorus 32–labeled DNA probes specific for the EBV genomic termini or for rearranged T cell receptor (TCR) were performed as described previously.[14,15] Autoradiography was carried out at –70°C for 1 to 7 days.

Heteroduplex Analysis of T-Cell Receptor-γ Gene Rearrangement

Amplification and heteroduplex analysis for TCR-γ gene rearrangement was performed as previously described,[16] with minor modifications. Consensus primers for the TCR V-J junction were used to amplify genomic DNA. Positive and negative controls were included in all polymerase chain reaction (PCR)

and heteroduplex reactions. The primer sequences were CACATCCACTGGTACCTACACCA for V1 and CCCGTCGACTACCTTGGAAATGTTGTATTCTTC for J1/2.

The PCR amplification of TCR-γ gene rearrangements was performed in a thermal cycler (model 2400; Perkin-Elmer, Foster City, CA), as follows. One hundred nanograms to 500 ng of genomic DNA was added to a reaction mixture containing 2.5 U Ampli Taq Gold polymerase (Perkin-Elmer), 10 pmol/L of each primer, 100 µmol/L of each deoxy nucleotide triphosphate, in buffer (Perkin-Elmer PCR buffer II; 10 mmol/L TRIS-hydrochloride, pH 8.3; 50 mmol/L potassium chloride) with 1.5 mmol/L magnesium chloride. After 95°C denaturation the TCR-γ was amplified by 20 cycles of PCR, each consisting of 40 seconds of denaturing at 95°C, 30 seconds of annealing at 65°C, decreasing by 1°C per cycle, and 30 seconds of extension at 72°C, followed by 15 cycles with the same denaturing and extension temperatures and an annealing temperature of 45°C, followed by a final 5-minute extension at 72°C.

The PCR products were first visualized on 2% agarose gel to document successful amplification. Then 20 µL of the PCR product with 2 µL of 0.05 mol/L EDTA added was heated to 95°C for 10 minutes, slowly cooled to 37°C over 30 minutes with the thermal cycler, and placed on ice. The samples were then electrophoresed on a mutation detection enhancement gel (FMC Bioproducts, Rocklands, ME) for 12 hours at 90V in TRIS-borate-EDTA buffer. Heteroduplex patterns were determined by staining with ethidium bromide and photography under ultraviolet light.

Results

Morphology and Immunohistochemistry

At initial examination, the blood films from patient 1 showed 30% to 40% blast forms with irregular nuclear contour and basophilic cytoplasm, some with azurophilic granules **Image 1A**. The bone marrow aspirate from patient 1 showed 70% to 80% blast forms with similar architecture **Image 1B**; likewise, the bone marrow biopsy specimen showed 70% to 80% cellularity, with 60% blastlike cells **Image 1C**.

The blood films from patient 2 demonstrated atypical large cells with irregular nuclear contours, relatively condensed chromatin, and abundant azurophilic granules in the cytoplasm **Image 2A**. A cytocentrifuge slide of the Ficoll-treated bone marrow aspirate from patient 2 revealed 40% to 50% similarly atypical cells **Image 2B**; and the bone marrow biopsy specimen showed 60% cellularity with occasional large atypical lymphoid cells but no lymphoid aggregates or diffuse infiltrates **Image 2C**.

The resected bowel segment from patient 2 was studded with multiple firm nodular masses ranging from 0.5 to 3.0 cm in greatest diameter, associated with ulceration and hemorrhage **Image 3A**. Histologic analysis revealed an extensive sheet-like infiltrate of atypical lymphocytes penetrating the entire thickness of the bowel wall. The infiltrate was particularly dense in the lamina propria and surrounding mucosal glands **Image 3B**. Focal glands also revealed intramucosal invasion by neoplastic cells **Image 3C**. The infiltrate was composed of large atypical lymphocytes with irregular nuclear outlines and abundant cytoplasm. Wright-Giemsa–stained touch preparations showed azurophilic granules scattered within the cytoplasm of these lymphocytes. Thirteen lymph nodes were identified in the surrounding adipose tissue, all of which exhibited involvement by lymphoma. Immunoperoxidase studies on sections of jejunum displayed strong expression of CD56 **Image 3D** and CD57, but no expression of CD20. These findings confirmed involvement of the jejunum and adjacent lymph nodes by NK-like T-cell lymphoma.

Flow Cytometry

Flow cytometry of the bone marrow from patient 1 showed a homogeneous population of T/NK cells, positive for CD2, CD5, CD8, CD56, and DR, but not CD3, CD4, CD7, CD16, CD57, and CD11c **Table 2**. However, the blast cells contained cytoplasmic CD3 (Leu-4), as demonstrated by slide immunocytochemistry on bone marrow aspirate cells **Image 4**. Flow cytometry of the peripheral blood showed a similar population of T/NK cells, but differed from the bone marrow in that approximately one third of the CD56-positive cells also weakly expressed surface CD3 (see Table 2). Similar to the bone marrow, slide immunophenotyping showed that the majority of the large cells were strongly positive for CD3 with Leu-4 antibody, suggesting T-cell lineage.

Flow cytometry of peripheral blood and bone marrow from patient 2 revealed a population of T/NK cells that expressed T-cell antigens CD3, CD2, CD7, and CD8 (partial, weak expression) and NK antigens CD56, CD57, and CD11c, but not pan-T antigens CD5 and CD4, and NK antigen CD16 (see Table 2). Neither TCR-αβ nor TCR-γδ heterodimers were expressed on the atypical lymphoid cells in the bone marrow. In both patients, the neoplastic cells were mature postthymic T cells, inasmuch as they lacked expression of terminal deoxynucleotidyl transferase.

Molecular Genetics

Southern blot analysis of the bone marrow cells from patient 1 revealed a clonal rearrangement of the TCR β chain. Heteroduplex analysis on blood cell samples from patient 2 showed clonal rearrangement of the TCR γ chain. These studies indicate malignant expansion of clonal T cells in both patients.

Cytogenetics

Chromosome analysis in patient 1 demonstrated an abnormal clone in all 20 cells, 47,XX,+1,add(8)(q24.3),

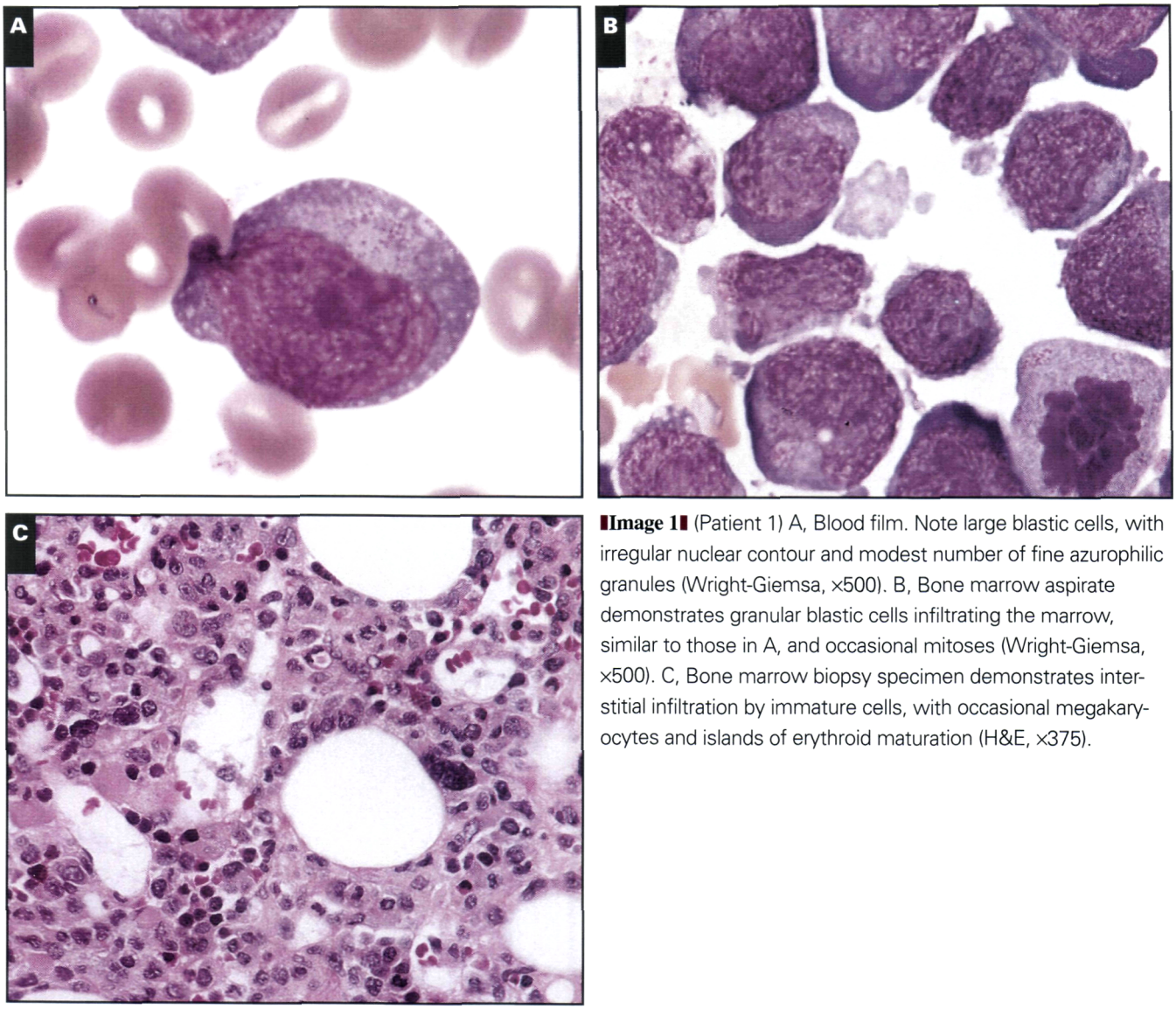

Image 1 (Patient 1) A, Blood film. Note large blastic cells, with irregular nuclear contour and modest number of fine azurophilic granules (Wright-Giemsa, ×500). B, Bone marrow aspirate demonstrates granular blastic cells infiltrating the marrow, similar to those in A, and occasional mitoses (Wright-Giemsa, ×500). C, Bone marrow biopsy specimen demonstrates interstitial infiltration by immature cells, with occasional megakaryocytes and islands of erythroid maturation (H&E, ×375).

i(19)(q10), characterized by trisomy 1, extra unidentified material on the long arm of chromosome 8, and an isochromosome for the long arm of chromosome 19. Eleven of these cells were characterized by only these abnormalities; 1 cell was missing chromosome 5; and the remaining 8 cells had additional nonclonal structural rearrangements, telomeric associations, or aneuploidies, suggesting karyotypic instability. Cytogenetic studies in patient 2 failed to reveal any karyotypic abnormality; however, only 4 cells could be analyzed. A clonal abnormality cannot be eliminated, because so few metaphases were available for analysis.

Detection of Epstein-Barr Virus

Patient 1 exhibited serologic evidence of recent EBV infection or reactivation, including a positive reaction (1:5,120) for early (diffuse) antibody and viral capsid IgG (1:20,480) with negative early (restricted) antibody (<1:5), viral capsid IgM (<1:10), and Epstein-Barr nuclear antibody (1:5). In situ hybridization studies for EBV performed on bone marrow revealed the presence of EBV mRNA within neoplastic cells. In patient 2, in situ hybridization studies of bone marrow failed to reveal EBV mRNA, and studies of jejunal tissue yielded equivocal findings. However, in patient 2, Southern blot analysis of bone marrow showed a faint band indicating clonal EBV genomes.

Discussion

The two cases of NK-like T-cell PTLD described are unusual in that a leukemic manifestation was the primary presentation of the malignancy. Patient 1 had minimal organ involvement, confirmed at postmortem examination. In patient 2, organ involvement was diagnosed 2 months after

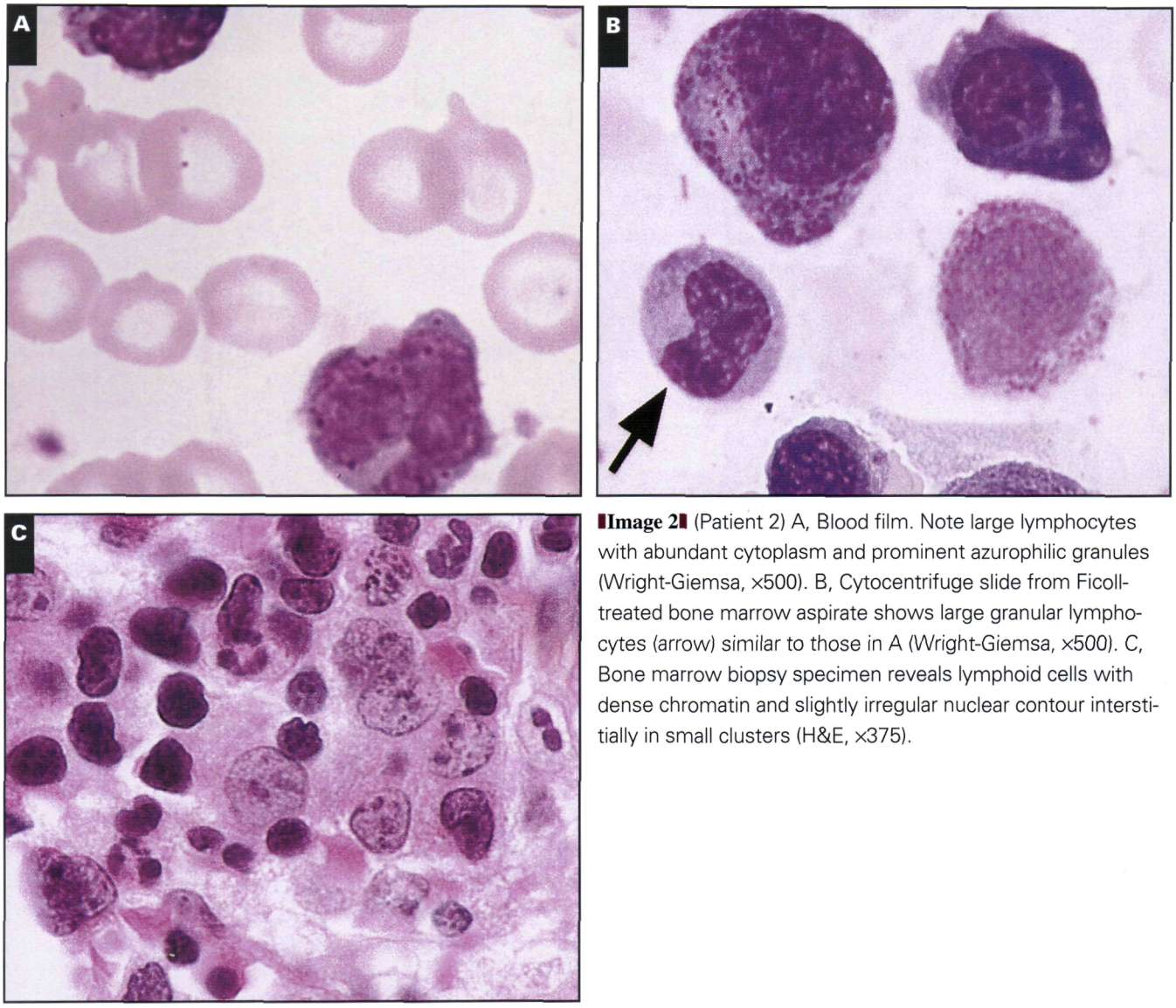

Image 2 (Patient 2) A, Blood film. Note large lymphocytes with abundant cytoplasm and prominent azurophilic granules (Wright-Giemsa, ×500). B, Cytocentrifuge slide from Ficoll-treated bone marrow aspirate shows large granular lymphocytes (arrow) similar to those in A (Wright-Giemsa, ×500). C, Bone marrow biopsy specimen reveals lymphoid cells with dense chromatin and slightly irregular nuclear contour interstitially in small clusters (H&E, ×375).

initial leukemic presentation. In patient 1, PTLD developed 7 years after heart-lung transplantation, whereas in patient 2 PTLD did not develop for an unusually long interval of 24 years after renal transplantation. Variable intervals between transplantation and development of PTLD have been reported for different allografts, ranging from a mean of 2.5 months in bone marrow transplantation[17,18] to a mean of 5.3 years in solid organ transplantation.[19] In a recent series of 21 post–cardiac transplantation lymphomas, the mean interval to development of PTLD was 9.3 years.[20]

The cytologic findings of the circulating cells was another unusual feature, particularly the marked nuclear irregularity of the large granular lymphocytes. At presentation, patient 1 was thought to have acute myelogenous leukemia because of the large numbers of circulating immature cells with azurophilic granules. However, a T/NK lineage for the neoplasm became apparent from the immunophenotyping results, which showed that although there was lack of immonoreactivity for both myeloid and myelomonocytic markers (CD11c, CD13, CD14, CD33, CD34), numerous T-cell and NK antigens were positive. Thus there is no support for myeloid/NK cell precursor acute leukemia.[21,22] In patient 2, an asymptomatic initial clinical presentation was more typical of an indolent T/NK LGL or reactive LGL lymphocytosis. However, the cytologic atypia of the circulating LGLs on routine blood films, together with an anomalous T/NK phenotype, was of concern for an aggressive variant of T-cell LGL and warranted close follow-up.

The presence of clonal TCR gene rearrangements in both of these malignancies is evidence for T-cell rather than NK-cell derivation. The heterogeneity of NK-like T-cell lymphomas with regard to rearrangement and expression of αβ and γδ TCR subtypes has been reported.[10,23] Our observations are analogous; we observed β and γ gene rearrangments in these 2 cases

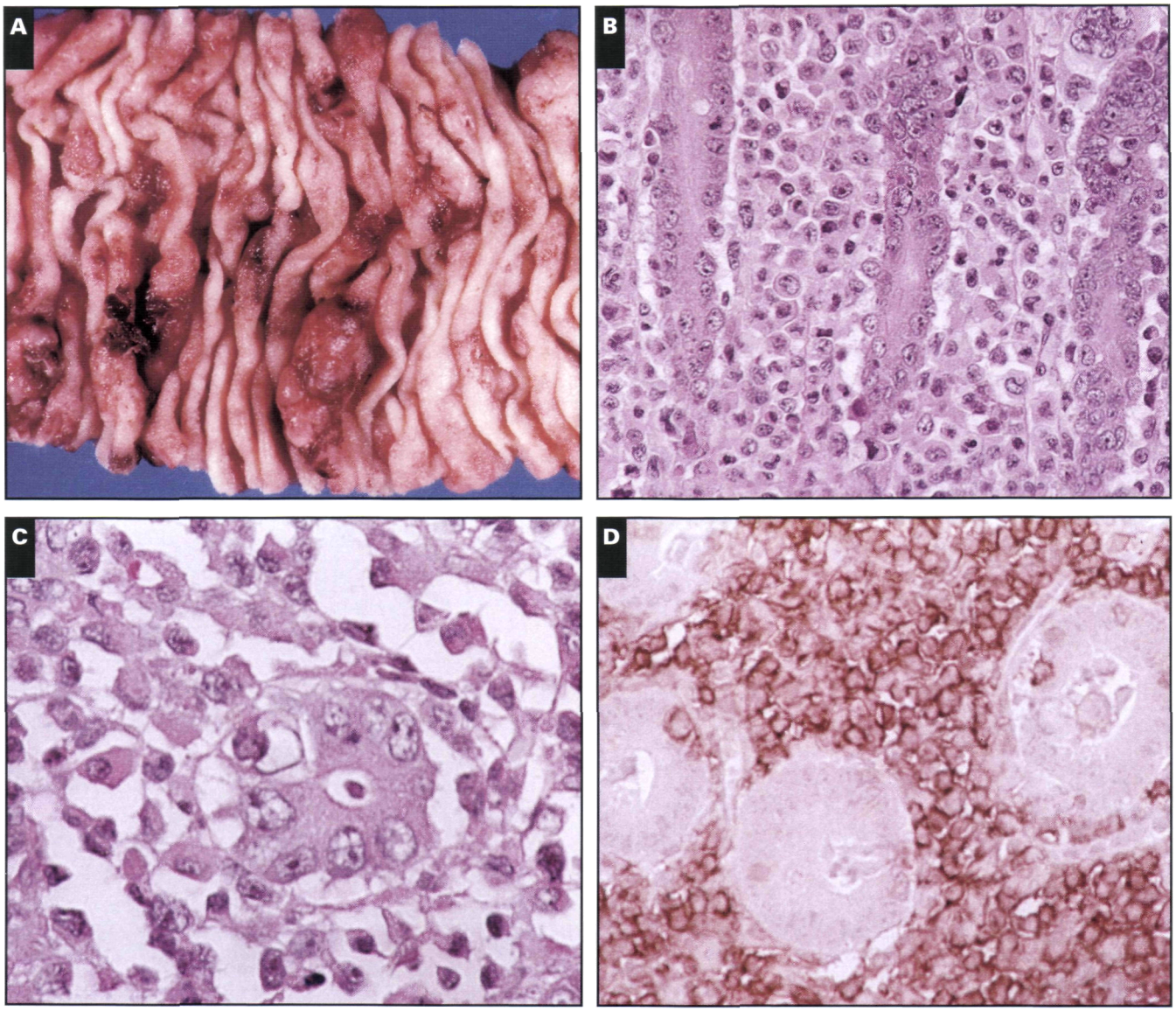

Image 3 (Patient 2) Resected jejunal segment. A, Note multiple nodular masses, associated with ulceration and hemorrhage (×1). B, Lymphoid infiltrate in bowel wall (H&E, ×150). C, Intramucosal invasion by neoplastic cells, with B lymphoepithelial appearance (H&E, ×250). D, Immunoperoxidase studies revealed strong positivity for CD56 (×250).

of posttransplantation NK-like T-cell leukemia. However, the malignant cells in patient 2 failed to express the framework TCR antigen, as indicated at flow cytometry analysis. Nonproductive TCR rearrangement is common in peripheral T-cell lymphomas, often with discordance between surface expression of CD3 and silent TCR.[24,25]

The heterogeneous presentations of NK-like T-cell malignancies render classification of these neoplasms complex. As described by Jaffe et al,[26] the differential diagnosis of such cases includes aggressive NK-like T-LGL leukemia or lymphoma, hepatosplenic γδ T-cell lymphoma, intestinal T-cell lymphoma, and chronic T-LGL (NK-like) leukemia. However, hepatosplenic γδ T-cell malignancies rarely show leukemic symptoms, and intestinal lymphomas seldom involve the bone marrow and peripheral blood. Furthermore, chronic NK-like T-LGL leukemia, including 1 case associated with orthotopic liver transplantation,[27] does not show atypical cell architecture or an aggressive clinical course, and usually has a $CD56^-$, $CD57^+$ immunophenotype. Thus aggressive NK-like T-LGL leukemia or lymphoma is the most likely diagnosis that encompasses the clinical, cytomorphologic, and immunologic features elaborated in our 2 cases.

Although aggressive NK-like T-LGL leukemia or lymphoma with an initial leukemic presentation has been described in immunocompetent patients,[28] massive lymphadenopathy and organomegaly were evident, features absent in our patients. Our findings in these 2 organ transplant recipients share significant similarities with aggressive NK-like T-cell

Table 2
Flow Cytometry*

Antibody	Patient 1 Blood	Patient 1 Bone Marrow	Patient 2 Blood	Patient 2 Bone Marrow
B lineage				
CD10	<1	<1	<1	<1
CD19	2	1	<1	1
CD20	2	<1	<1	1
T/NK lineage				
CD2	99	87	80	68
CD3	55	19	83	59
CD4	14	3	3	4
CD5	93	88	8	10
CD7	35	6	94	74
CD8	83	84	39	28
CD16	<1	<1	<1	2
CD56	63	85	87	72
CD57	2	<1	78	67
βF1	NP	NP	10	NP
TCR-δ1	NP	NP	2	NP
Myelomonocytic				
CD11c	1	1	49	35
CD13	1	1	1	5
CD14	<1	<1	NP	NP
CD33	1	1	NP	NP
CD34	<1	<1	NP	NP
Other				
DR	62	77	NP	NP

NP = not performed.
*Data represent percentage of events positive in C45-positive lymphoid light scatter analysis gate.

Table 3
Summary of Epstein-Barr Virus, Cytogenetic, and Molecular Diagnostic Studies

Analysis	Patient 1	Patient 2
Epstein-Barr virus serology	Positive	Negative
Southern blot	NP	Faint clonal bands
In situ hybridization	Positive	Equivocal
Cytogenetics	47,XX,+1,add (8)(q24.3), i(19)(q10)	ND
TCR-αβ gene Southern blot	Rearranged	Germ line
TCR-γ gene PCR-heteroduplex	NP	Rearranged

NP = not performed; ND = not detected; TCR = T-cell receptor.

malignancies in 4 immunosuppressed patients reported by Macon et al.[10] The LGL proliferations showed $CD3^+$, $CD56^+$ expression, and both αβ and γδ T-cell phenotypes were observed.[29] Atypical cytologic findings of marked nuclear pleomorphism or blastlike architecture were described, which rarely are seen in chronic, indolent LGL leukemias. In 3 of 4 immunosuppressed patients, a leukemic phase was part of the disease spectrum, although not initially. Likewise, a leukemic presentation was rare in the posttransplantation T-cell lymphoma cases reviewed by van Gorp et al.[6]

Association with EBV infection is important in the pathogenesis of B-cell PTLD, but has been inconsistently demonstrated in PTLD with T-cell lineage.[4,6] Two of the 4 posttransplant

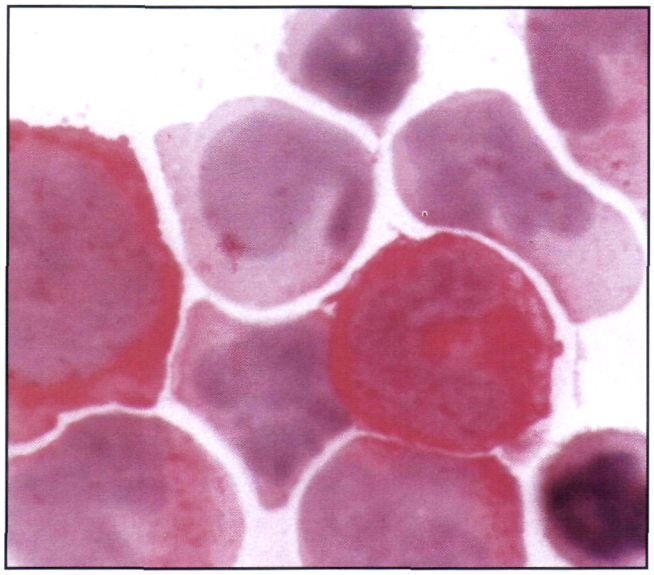

Image 4 (Patient 1) Ficoll-treated bone marrow aspirate, cytocentrifuge slide. Slide immunophenotyping with avidin–alkaline phosphatase amplification shows that many of the neoplastic T/NK lymphoid cells express cytoplasmic CD3 (×500).

NK-like T-cell malignancies studied by Macon et al[10] demonstrated strong LMP immunoreactivity, supporting the presence of EBV in leukemic cells. In patient 1, we observed serologic evidence of a recent EBV infection or reactivation, and EBV mRNA in neoplastic cells in the bone marrow. In patient 2, we found very weak EBV clonality, which may represent a minor population of infected cells. However, it is unclear from these data whether EBV plays a pathogenic role in the genesis or evolution of NK-like T-cell leukemias. We speculate that these T/NK malignancies could arise from deregulation of reactive, stimulated cytotoxic T cells generated in response to EBV infection of B lymphocytes. Coinfection of the reactive T cells with other viruses prevalent in the immunosuppressed host, such as human herpesvirus 6, may be an additional carcinogenic event in the genesis of these malignancies.

The abnormal karyotype in patient 1, 47,XX,+1, add(8)(q24.3),i(19)(q10), is interesting because of potential involvement of the c-*myc* gene located at 8q24. The c-*myc* oncogene rearrangement may play a role in development of PTLD; deregulation of c-*myc* has been reported in T-cell leukemias[30] and may be associated with disease progression in EBV-related B-cell PTLD.[4] One of 2 immunosuppressed patients with karyotypic analysis reported by Macon et al[10] also had a translocation involving the 8q24 breakpoint, but no detectable c-*myc* rearrangement. Of further interest in patient 1 is the presence of trisomy 1, a secondary acquired change that may represent karyotypic evolution. This karyotypic evolution of the malignant clone may be paralleled by immunophenotypic evolution, characterized by the loss of surface CD3 in the bone marrow cells and a portion of the blood cells.

It is important to recognize that NK-like T-cell malignancies are part of the spectrum of PTLDs that complicate long-term immunosuppression, and may occur in posttransplantation settings. Our observations in 2 organ transplant recipients indicate that NK-like T-cell malignancies may present with a leukemic phase. The phenotypic, cytologic, and cytogenetic parameters are key to establishing a diagnosis and differentiating these aggressive disorders from reactive LGL proliferations.

From the Department of Pathology, Stanford University School of Medicine, Stanford, CA.

Address reprint requests to Dr Natkunam: Department of Pathology, Stanford University Medical Center, 300 Pasteur Dr, Stanford, CA 94305-5302.

Acknowledgments: We thank Athena Milatovich-Cherry, PhD, Cytogenetics Laboratory, Stanford Health Services, for review and interpretation of the cytogenetic findings.

References

1. Hanto DW, Frizzera G, Purtilo DT, et al. Clinical spectrum of lymphoproliferative disorders in renal transplant recipients and evidence for the role of Epstein-Barr virus. *Cancer Res*. 1981;41:4253–4261.
2. Hanto DW, Gajl-Peczalska KJ, Frizzzera G, et al. Epstein-Barr virus induced polyclonal and monoclonal B-cell lymphoproliferative diseases occurring after renal transplantation: clinical, pathologic, and virologic findings and implications for therapy. *Ann Surg*. 1983;198:356–369.
3. Frizzera G, Hanto DW, Gajl-Peczalska KJ, et al. Polymorphic diffuse B-cell hyperplasias and lymphomas in renal transplant recipients. *Cancer Res*. 1981;41:4262–4279.
4. Craig FE, Gulley ML, Banks PM. Posttransplantation lymphoproliferative disorders. *Am J Clin Pathol*. 1993;99:265–276.
5. Knowles DM, Cesarman E, Chadburn A, et al. Correlative morphology and molecular genetic analysis demonstrates three distinct categories of posttransplantation lymphoproliferative disorders. *Blood*. 1995;85:552–565.
6. Van Gorp J, Doornewaard H, Verdonck LF, et al. Posttransplant T-cell lymphoma: report of three cases and a review of the literature. *Cancer*. 1994;73:3064–3072.
7. Shiong YS, Lian JD, Lin CY, et al. Epstein-Barr virus–associated T-cell lymphoma of the maxillary sinus in a renal transplant recipient. *Transplant Proc*. 1992;24:1929–1931.
8. Kumar S, Kumar D, Kingma DW, et al. Epstein-Barr virus associated T-cell lymphoma in a renal transplant patient. *Am J Surg Pathol*. 1993;17:1046–1053.
9. Waller EK, Ziemianska M, Bangs CD, et al. Characterization of posttransplant lymphomas that express T-cell-associated markers: immunophenotypes, molecular genetics, cytogenetics, and heterotransplantation in severe combined immunodeficient mice. *Blood*. 1993;82:247–261.
10. Macon WR, Williams ME, Greer JP, et al. Natural killer-like T cell lymphomas: aggressive lymphomas of T-large granular lymphocytes. *Blood*. 1996; 87:1474–1483.
11. Bindl JM, Warnke RA. Advantages of detecting monoclonal antibody binding to tissue sections with biotin and avidin reagents in Coplin jars. *Am J Clin Pathol*. 1986;85:490–493.
12. Van de Rijn M, Cleary ML, Variakojis D, et al. Epstein-Barr virus clonality in lymphomas in patients with rheumatoid arthritis. *Arthritis Rheum*. 1996;39:638–642.
13. Barch MJ, ed. *ACT Cytogenetics Laboratory Manual*. 2nd ed. New York, NY: Raven Press; 1991:222.
14. Cleary ML, Chao J, Warnke R, et al. Immunoglobulin gene rearrangement as a diagnostic criterion of B cell lymphoma. *Proc Natl Acad Sci U S A*. 1984;81:593–597.
15. Cleary ML, Nalesnik MA, Shearer WT, et al. Clonal analysis of transplant-associated lymphoproliferations based on the structure of the genomic termini of the Epstein-Barr virus. *Blood*. 1988;72:349–352.
16. Bottaro M, Berti E, Biondi A, et al. Heteroduplex analysis for T-cell receptor γ gene rearrangement for diagnosis and monitoring of cutaneous T-cell lymphomas. *Blood*. 1994;83:3271–3278.
17. Zutter MM, Martin PJ, Sale GE, et al. Epstein-Barr virus lymphoproliferation after bone marrow transplantation. *Blood*. 1988;72:520–529.
18. Shapiro RS, McClain K, Frizzera G, et al. Epstein-Barr virus–associated lymphoproliferation after bone marrow transplantation. *Blood*. 1988;71:1234–1243.
19. Hanto DW, Frizzera G, Gajl-Peczalska KJ, et al. Epstein-Barr virus, immunodeficiency, and B cell lymphoproliferation. *Transplantation*. 1985;39:461–472.
20. Kowal-Vern A, Swinnen L, Pyle J, et al. Characterization of postcardiac transplant lymphomas: histology, immunophenotyping, immunohistochemistry, and gene rearrangement. *Arch Pathol Lab Med*. 1996;120:41–48.
21. Scott AA, Head DR, Kopecky KJ, et al. HLA-DR–, CD33+, CD56+, CD16– myeloid/natural killer cell acute leukemia: a previously unrecognized form of acute leukemia potentially misdiagnosed as French-American-British acute myeloid leukemia–M3. *Blood*. 1994;84:244–255.
22. Suzuki R, Yamamoto K, Seto M, et al. CD7+ and CD56+ myeloid/natural killer cell precursor acute leukemia: a distinct hematolymphoid disease entity. *Blood*. 1997;90:2417–2428.
23. Sun T, Schulman P, Kolitz J, et al. A study of lymphoma of large granular lymphocytes with modern modalities: report of two cases and review of the literature. *Am J Hematol*. 1992;40:135–145.
24. Emile JF, Boulland ML, Haioun C, et al. CD5– CD56+ T-cell receptor silent peripheral T-cell lymphomas are natural killer cell lymphomas. *Blood*. 1996;87:1466–1473.
25. Picker LJ, Brenner MB, Michie S, et al. Expression of T cell receptor delta chains in benign and malignant T lineage lymphoproliferations. *Am J Pathol*. 1988;132:401–405.
26. Jaffe ES, Chan JKC, Su IJ, et al. Report of the Workshop on Nasal and Related Extranodal Angiocentric T/NK lymphomas: definitions, differential diagnosis, and epidemiology. *Am J Surg Pathol*. 1996;20:103–111.
27. Gentile TC, Uner AH, Hutchison RE, et al. CD3+ CD56+ aggressive variant of large granular lymphocyte leukemia. *Blood*. 1994;84:2315–2321.
28. Feher O, Barilla D, Locker J, et al. T-cell large granular lymphocytic leukemia following orthotopic liver transplantation. *Am J Hematol*. 1995;49:216–220.
29. Jaffe ES. Classification of natural killer (NK) cell and NK-like T-cell malignancies. *Blood*. 1996;87:1207–1210.
30. Erickson J, Finger L, Sun L, et al. Deregulation of c-*myc* by translocation of the alpha-locus of the T-cell receptor in T-cell leukemias. *Science*. 1986;232:884–886.

HOLOGIC®

First and Only FDA Cleared
Digital Cytology System

Genius™ Cervical AI

Genius™ Review Station

Genius™ Digital Imager

Empower Your Genius With Ours

Make a Greater Impact on Cervical Cancer
with the Advanced Technology of the
Genius™ Digital Diagnostics System

Click or Scan
to discover more

genius™
DIGITAL DIAGNOSTICS